



Multi Input DC-DC Converters and Mitigation of Loop Interactions Using Decoupled Control

Smrithi Lakshmi M, Dr. Devi V

M. Tech in PE(EEE), NSS College of Engineering, Palakkad, Kerala, India

Principal and Professor, Dept. of EEE, Royal College of Engineering and Technology, Kerala, India

ABSTRACT: Electric Vehicles (EVs) can be powered through conventional methods as well as through renewable energy resources. But energy production through solar depends on the environmental conditions like irradiation level, temperature, orientation of panel and unpredictable shadows. So, it has to be supplemented to meet the load requirement whenever required. Fuel Cell (FC) together with Photo Voltaic (PV) cells and battery, incorporated with suitable interface converter is proposed here making the system reliable. But the control of Multi Input Converter (MIC) is quite difficult because of the interactions in the feedback control loops, which affects the system performance. To mitigate such interactions, decoupling network is proposed. The performance enhancement with decoupling control is validated through simulations and hardware results.

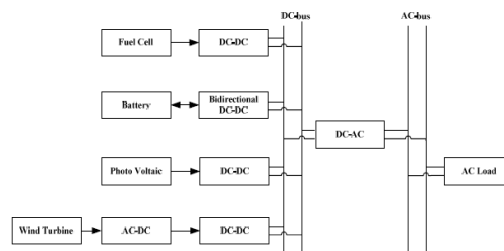
KEYWORDS : Multi Input Converter (MIC), Decoupling network, Photo Voltaic (PV), Electric Vehicles (EVs), Multi variable system, Dynamic modelling

I. INTRODUCTION

To reduce Carbon dioxide (CO₂) emissions as well as other harmful environmental pollutants, Zero Emission Vehicles (ZEVs) are coming up. They have fewer moving parts and minimum maintenance. EV can be powered using battery and from renewable energy resources like solar. But due to intermittency of renewable sources, supplementing with sources like FC which is environmental friendly has become an important research area [1].

II. MULTI INPUT CONVERTERS

In most power electronic systems, input power or output demand may subject to instantaneous changes. Hence additional energy sources may be required to meet the increased load demand to maintain reliability. Therefore, multiple power electronic converters are used to connect multiple sources as a single system, in order to meet the load demand [2,3]. Different configurations are there to incorporate multiple sources to the system under consideration. [4]. In conventional parallel connected converters, multiple converters are connected in parallel. The main drawbacks of such systems are, its inherent complexity and high cost due to multiple conversion stages [5-9]. As different sources have different voltage levels, they cannot be connected in parallel directly.



(a)

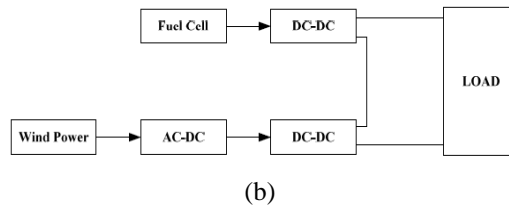


Fig 1 Conventional converter connection(a)Parallel (b)Series

Inconventional series connected converters, DC-DC converters are connected in series to the load and are controlled independently. The main disadvantage of such a system is high power loss, as the output current flows through both the converters. Sources connected in series have to conduct same current which is not always desirable [10]. Connecting converters in parallel or series results in use of a greater number of devices, more losses and lesser efficiency. Hence use of a single, MIC is preferred over several multiple converters to obtain the same action.

One method of deriving MICs is based on principle of flux additivity. In this method sources are interconnected using a multiwinding transformer [11,12]. Here, instead of combining energy sources in the electric form, they are combined in the magnetic form, together in the magnetic core of the coupled transformer by adding up their produced magnetic flux. But here bidirectional capability is not incorporated.

Bidirectional capability can be achieved by combining DCLink and magnetic coupling [13,14]. This type of converter is of simple topology and have minimum number of power devices [15]. The major disadvantage of converters using multiwinding transformer is that as the voltage rating increases, the size of transformer increases which increases the converter size. Hence among different MIC configurations, the one without transformers – non isolated MICs - is usually preferred. [16] These converters can accommodate arbitrary number of sources and loads and can be structured in different ways [17]. All the inputs can deliver the load individually or simultaneously with lesser number of components and with bidirectional capability [18].

General form of a MICs is shown in Fig 2.

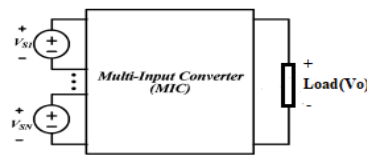


Fig 2 General form of MICs

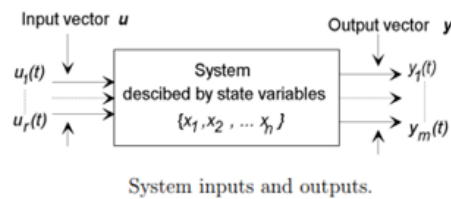
As we are using more than one source of different types in these types of converter, it should be proficient in energy diversification. The source inclusion to this MIC is according to the structure of the converter. It should manage and control power flow to the load based on requirement. Hence control systems for these converters are complex. A MIC has to be treated as a MIMO system which is nonlinear, imprecisely known multivariable with many interactions.

2.1 Multi Variable Systems

A system having single input, single output and can be controlled by a single variable is named as a single variable system. Systems with more than one control variable is called multi variable system. Examples of multivariable systems are a heated liquid tank where both the level and the temperature are to be controlled, a robot manipulator where the positions of the manipulators (arms) are to be controlled, and a chemical reactor where concentration and temperature are the control parameters [19]. Multi variable system are large dimensioned system, as dimension depends on the number of system variables chosen [19].

2.2 Multi variable System representation

For the sake of simplicity, the large dimensioned systems can often be decomposed to sets of smaller dimensioned systems [19]. A multi input output system is shown in Fig 3a.



System inputs and outputs.

(a)

Fig 3. MIMO system

Multi variable systems are having two types of representations namely P-canonical representation and V-canonical representation [19].The structural difference between the two is that in P-canonical representation, loop interactions are represented as feedforward couplings where as in the V-canonical representation, loop interactions are represented as feedback couplings. The elements within the blocks of the diagram are transfer functions which defines the relationship between the respective inputoutput pairs.

P-canonical representation of a 2x2 system is shown in Fig 4.

Where, $G_{11} = \frac{y_1}{u_1}$, $G_{21} = \frac{y_2}{u_1}$, $G_{12} = \frac{y_1}{u_2}$, $G_{22} = \frac{y_2}{u_2}$ and y_1 and y_2 are outputs for inputs u_1 and u_2 respectively.

On a loop by loop basis, the outputs of the system are related to input as:

$$y_1 = u_1 G_{11}^P + u_2 G_{12}^P \tag{1}$$

$$y_2 = u_1 G_{21}^P + u_2 G_{22}^P \tag{2}$$

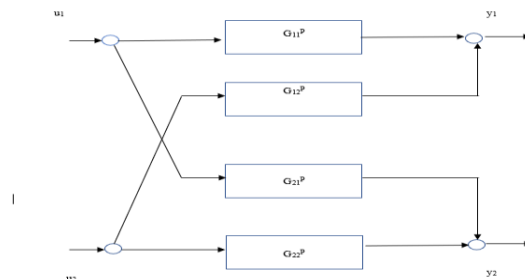


Fig 4. P-canonical representation of a 2x2 system

V-canonical representation of a 2x2 system is shown in Fig 5.

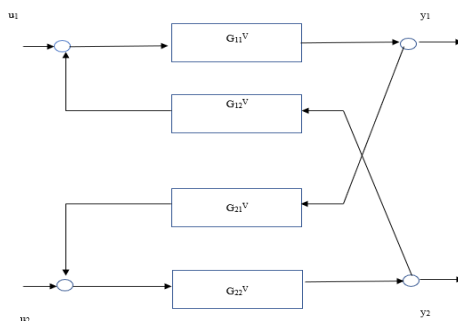


Fig 5. V-canonical representation of a 2x2 system

On a loop by loop basis, the input output notation is:

$$y_1 = [y_2 G_{12}^V + u_1] G_{11}^V \tag{3}$$

$$y_2 = [y_1 G_{21}^V + u_2] G_{22}^V \tag{4}$$

The factors that to be considered[4] to determine the choice of system representation are:

1. Model parameters, determined from experiments.



2. The model representing the process in simple form.
3. The model providing relevant information of the control system design.

In P-canonical form the elements of transfer function can be found from open loop experiments, therefore, P- canonical form is preferred.

III. PROPOSED MULTI INPUT DC-DC CONVERTER

Consider the three input DC-DC converter in Fig 6. The three inputs selected are PV, FC and Lead Acid battery. This converter utilizes four switches S_1, S_2, S_3 and S_4 . V_1 is the PV panel output voltage, V_2 is FC voltage, V_B is Battery voltage. L_1 and L_2 are inductors with internal resistances r_1 and r_2 , C is capacitor and R_L is the load resistance.

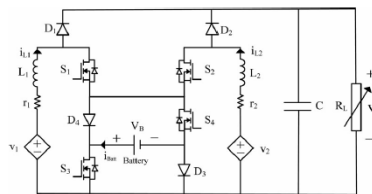
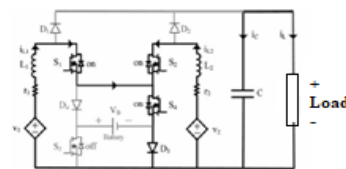


Fig 6. Circuit diagram of proposed converter

There are three modes of operation for the converter: supplying the load through two input sources without battery, supplying the load with two input sources together with the battery and supplying the load with two input sources with battery being charged. Each mode has more than one switching states in order to regulate the output voltage to the required magnitude-

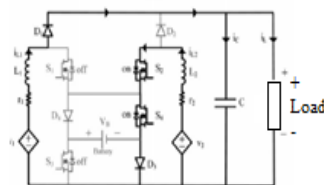
In mode 1 there are 3 switching states with switch S_4 being ON throughout. In state 1 Switches S_1, S_2 are turned ON in order to charge L_1 and L_2 with voltages V_1 and V_2 for maintaining load voltage.



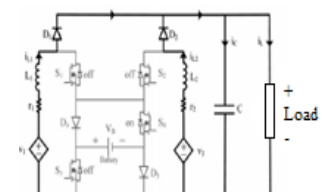
(a)

In state 2 Switches S_1 is turned OFF and S_2 is kept ON. So inductor L_1 is discharged to supply the load with voltage across L_1 being $V_1 - V_0$. Inductor L_2 is still charged with voltage V_2 .

In state 3 Switches S_1 and S_2 are OFF, so that L_2 and L_1 will be discharging with voltage across $V_2 - V_0$ and $V_1 - V_0$ to supply the load.



(b)



(c)

Fig 7a,7b,7c Circuit diagram of switching state 1,2,3 in Mode

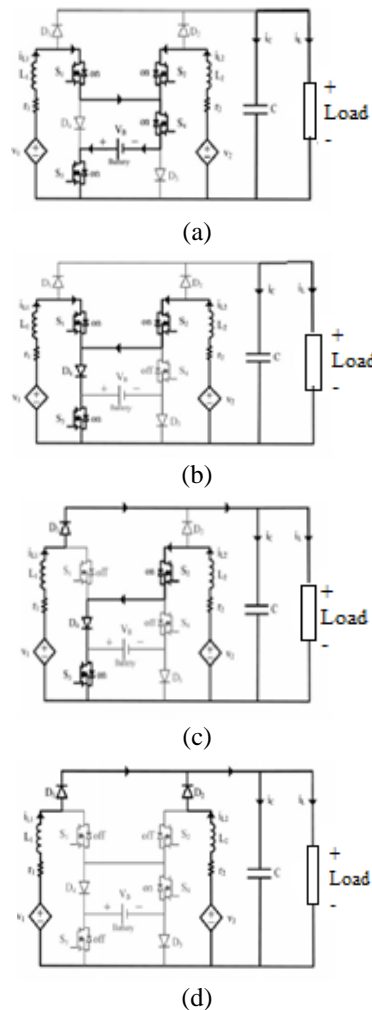


Fig 8a,8b,8cand 8d Circuit diagram of switching state 1,2,3and 4 in Mode 2

In mode 2 there are 4 switching states for making the system to supply the load with required voltage.

In state 1 of mode 2 Switches S_1 , S_2 , and S_4 are turned ON so that inductors L_1 and L_2 will be charged with voltages $V_1 + V_B$ and $V_2 + V_B$ respectively where V_B is the battery voltage. In this mode capacitor is discharged to supply the load.

In state 2 switches S_1 , S_2 are kept ON and S_4 is turned OFF. So inductors L_1 and L_2 are charged with voltages V_1 and V_2 respectively. Capacitor is discharged to supply the load.

In state 3 switches S_1 is turned OFF and S_2 is kept ON. So inductor L_1 is discharged to supply the load with voltage across L_1 being $V_1 - V_0$. Inductor L_2 is still charged with voltage V_2 .

In state 4 Switches S_1 and S_2 are OFF, so that L_2 and L_1 will be discharging with voltage across $V_2 - V_0$ and $V_1 - V_0$ to supply the load.

In mode 3 there are 4 switching states for making the system to supply the load with required voltage.

In state 1 of mode 3 Switches S_1 , S_2 , and S_3 are turned ON So that inductors L_1 and L_2 will be charged with voltages V_1 and V_2 respectively. In this mode Capacitor is discharged to supply the load.

In state 2 Switches S_1 , S_2 are kept ON and S_3 is turned OFF and battery will be charging. Capacitor is discharged to supply the load.

In state 3 Switches S_1 is turned OFF and S_2 is kept ON. So inductor L_1 is discharged to supply the load with voltage across L_1 being $V_1 - V_0$. Inductor L_2 is still charged with voltage V_2 .

In state 4 Switches S_1 and S_2 are OFF, so that L_2 and L_1 will be discharging with voltage across $V_2 - V_0$ and $V_1 - V_0$ to supply the load.



In all modes of operation, the switches can be controlled independently with four different duty ratios, for controlling the power flow from input sources to output load. Power to the load can be delivered by the sources individually or simultaneously [1].

The three-input converter is operating in such a way that output voltage (V_o) is always maintained constant in all modes of operations. The converter will work as a three input DC-DC boost converter during three modes of operations on an average gain of 2.

Wave form of inductor current is shown in Fig 10. The inductor will be charged and discharged according to the switching operation. For the ease of explanation an R_L load is used, which is replaced by a BLDC motor used for EV applications during simulation and hardware part of the project work. BLDC motor is commonly used in EVs due its advantages such as low maintenance, efficiency, high operating speeds, no brush sparking, compact size and quick response.

For the different modes of MIC, controlling is difficult due to interactions and interdependence of the control loop variables which are the duty ratios. This affects the performance of the converter and thus output response is degraded. To avoid such interactions decoupling networks are suggested. Decoupling network can cancel out these interactions and thus the effect on the performance of the system can be reduced.

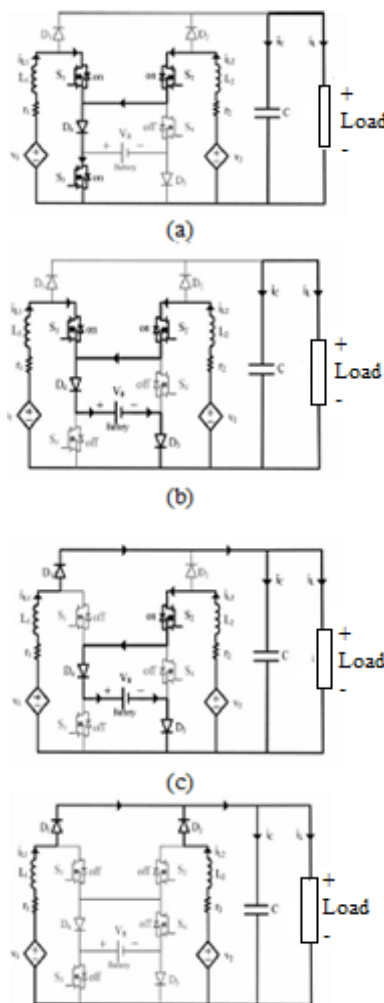


Fig 9a,9b,9c,9d Circuit diagram of switching state 1,2,3,4 in Mode3

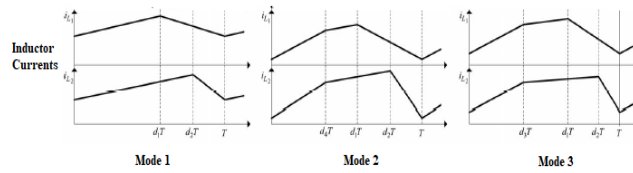


Fig 10. Inductor current

IV. MODELLING OF THREE INPUT CONVERTER

The proposed three input DC-DC converter has three different modes of operations. In order to regulate the input sources to maintain output voltage as desired, the converter needs to be controlled in each operation mode by controlling different control variables. First operation mode utilizes two active duty ratios, while in the second and third operation mode three different duty ratios are needed. Therefore, the three-input converter is to be treated as a Multi Input Multi Output (MIMO) control system. A multi loop system is shown in Fig 11[19].

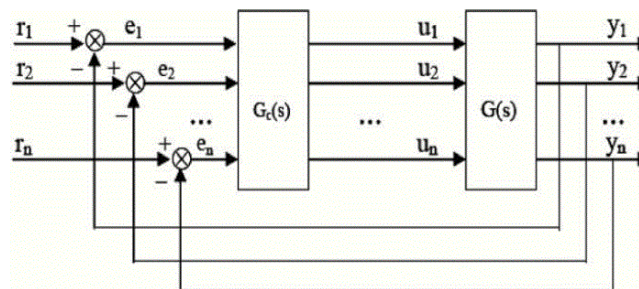


Fig 11 Multi loop systems

In order to design closed loop controllers for the proposed MIC with reduced interactions, a new control strategy is to be developed. For that the first step is obtain small-signal state space dynamic model including internal resistance of inductor [20].

The state space models are of the form

$$\dot{x} = A x + B u, y = C x + D u$$

Where x =state variable vector = $x_1, x_2, x_3 = \begin{bmatrix} i_{L1} \\ i_{L2} \\ V_o \end{bmatrix}$

u =control variable vector = u_1, u_2, u_3

y =output variable vectory = $[V_o]$

D matrix is '0'(zero) because this system does not contain a direct feed forward path. The control variables are the duty ratios d_1, d_2, d_3 and d_4 . ($u_1 u_2 u_3 u_4$)

As mentioned in section 1, in mode 1, three state variables are controlled by two control variables d_1 and d_2 . Applying KVL to Fig 7 (a) (b) (c) the differential equations for mode 1 are

$$L_1 \frac{di_{L1}}{dt} = d_1 v_1 + (1- d_1) (v_1 -v_0) - r_1 i_{L1} (5)$$

$$L_2 \frac{di_{L2}}{dt} = d_2 v_2 + (1- d_2) (v_2 -v_0) - r_2 i_{L2} (6)$$

$$C \frac{dv_0}{dt} = (1-d_1) i_{L1} + (1-d_2) i_{L2} - v_0 / R_L (7)$$

From Fig 8 (a) (b) (c) (d) (operation in diagram (a) and (b) are combined) the three control variables $d_1, d_2,$ and d_4 are controlled to regulate all three state variables. Differential equations for mode 2 are

$$L_1 \frac{di_{L1}}{dt} = v_1 (d_1 - d_4) + d_4 (v_1 - v_B) + (1 - d_1) (v_1 - v_0) - r_1 i_{L1} (8)$$

$$L_2 \frac{di_{L2}}{dt} = d_4 (v_2 - v_B) + (d_2 - d_4) v_2 + (1 - d_2) (v_2 - v_0) - r_2 i_{L2} (9)$$



$$C \frac{dv_0}{dt} = (1 - d_1) i_{L1} + (1 - d_2) i_{L2} - v_0 / R_L \tag{10}$$

In the third operation mode, Fig 9 (a) (b) (c) (d) (operation in diagram (a) and (b) are combined) three control variables $d_1, d_2,$ and d_3 are controlled to regulate all three state variables. Differential equations for mode 3 are

$$L_1 \frac{di_{L1}}{dt} = d_3 v_1 + (d_1 - d_3)(v_1 - v_B) + (1 - d_1)(v_1 - v_0) - r_1 i_{L1} \tag{11}$$

$$L_2 \frac{di_{L2}}{dt} = d_3 v_2 + (d_2 - d_3)(v_2 - v_B) + (1 - d_2)(v_2 - v_0) - r_2 i_{L2} \tag{12}$$

$$C \frac{dv_0}{dt} = (1 - d_1) i_{L1} + (1 - d_2) i_{L2} - v_0 / R_L \tag{13}$$

Substituting state variables to the differential equations (5) to (13) non linear statespace equations for the three modes can be formed [21]. In order to obtain linearized state space averaged equations, let us assume that the state and source variables is comprising of DC values ($\bar{X} \bar{D} \bar{V}$) and perturbations ($\tilde{x} \tilde{d} \tilde{v}$). Hence,
 $x = \bar{X} + \tilde{x}$, $d = \bar{D} + \tilde{d}$ and $v = \bar{V} + \tilde{v}$

Substituting perturbations to equations (5) to (13) and assuming that the perturbations are small and neglecting second and higher order terms will result in linearized state space models for different modes. Thus the state, source and output coefficient matrices are obtained as follows,

For ,Mode 1:

$$A = \begin{bmatrix} \frac{-r_1}{L_1} & 0 & \frac{D_1 - 1}{L_1} \\ 0 & \frac{-r_2}{L_2} & \frac{D_2 - 1}{L_2} \\ \frac{1 - D_1}{C} & \frac{1 - D_2}{C} & \frac{-1}{R_L C} \end{bmatrix} \quad B = \begin{bmatrix} \frac{V_0}{L_1} & 0 \\ 0 & \frac{V_0}{L_2} \\ \frac{-i_{L1}}{C} & \frac{-i_{L2}}{C} \end{bmatrix} \quad C = \begin{bmatrix} 1 & 0 & 0 \\ 0 & 0 & 0 \\ 0 & 0 & 1 \end{bmatrix}$$

Mode 2:

$$A = \begin{bmatrix} \frac{-r_1}{L_1} & 0 & \frac{D_1 - 1}{L_1} \\ 0 & \frac{-r_2}{L_2} & \frac{D_2 - 1}{L_2} \\ \frac{1 - D_1}{C} & \frac{1 - D_2}{C} & \frac{-1}{R_L C} \end{bmatrix} \quad B = \begin{bmatrix} \frac{V_0}{L_1} & 0 & \frac{V_B}{L_1} \\ 0 & \frac{V_0}{L_2} & \frac{V_B}{L_2} \\ \frac{-i_{L1}}{C} & \frac{-i_{L2}}{C} & 0 \end{bmatrix} \quad C = \begin{bmatrix} 1 & 0 & 0 \\ 0 & 1 & 0 \\ 0 & 0 & 1 \end{bmatrix}$$

Mode 3:

$$A = \begin{bmatrix} \frac{-r_1}{L_1} & 0 & \frac{D_1 - 1}{L_1} \\ 0 & \frac{-r_2}{L_2} & \frac{D_2 - 1}{L_2} \\ \frac{1 - D_1}{C} & \frac{1 - D_2}{C} & \frac{-1}{R_L C} \end{bmatrix} \quad B = \begin{bmatrix} \frac{V_0 - V_B}{L_1} & 0 & \frac{V_B}{L_1} \\ 0 & \frac{V_0 - V_B}{L_2} & \frac{V_B}{L_2} \\ \frac{-i_{L1}}{C} & \frac{-i_{L2}}{C} & 0 \end{bmatrix} \quad C = \begin{bmatrix} 1 & 0 & 0 \\ 0 & 1 & 0 \\ 0 & 0 & 1 \end{bmatrix}$$

Where, D_1 and D_2 represents the steady state part of duty ratios d_1 and d_2 respectively.

Using these matrices, we can obtain the transfer function of the MIC in mode 1, mode 2 and mode 3 using $G = C (sI - A)^{-1} B + D$, where G is the transfermatrix.

The obtained output input relation in mode 1 is;

$$[y] = \begin{bmatrix} g_{11} & g_{12} \\ g_{21} & g_{22} \end{bmatrix} \begin{bmatrix} d_1 \\ d_2 \end{bmatrix} \tag{14}$$

With Transfer function matrix for mode 1 as $G = \begin{bmatrix} g_{11} & g_{12} \\ g_{21} & g_{22} \end{bmatrix}$

In mode 2 is;

$$[y] = \begin{bmatrix} g_{11} & g_{12} & g_{13} \\ g_{21} & g_{22} & g_{23} \\ g_{31} & g_{32} & g_{33} \end{bmatrix} \begin{bmatrix} d_1 \\ d_2 \\ d_4 \end{bmatrix} \tag{15}$$



And Transfer function matrix is $G = \begin{bmatrix} g_{11} & g_{12} & g_{13} \\ g_{21} & g_{22} & g_{23} \\ g_{31} & g_{32} & g_{33} \end{bmatrix}$

In mode 3 is;

$$[y] = \begin{bmatrix} g_{11} & g_{12} & g_{13} \\ g_{21} & g_{22} & g_{23} \\ g_{31} & g_{32} & g_{33} \end{bmatrix} \begin{bmatrix} d_1 \\ d_2 \\ d_3 \end{bmatrix} \quad (16)$$

Transfer function matrix is $G = \begin{bmatrix} g_{11} & g_{12} & g_{13} \\ g_{21} & g_{22} & g_{23} \\ g_{31} & g_{32} & g_{33} \end{bmatrix}$

Using equations (14) to (16) we have to derive the transfer function matrix of decoupled network which is to be cascaded with the original system to reduce the impact of loop interactions or cross couplings in the system.

V. FORMULATION OF DECOUPLING NETWORK

Consider a system with two first order delay free processes G_{11} and G_{22} with proportional controls as shown in Fig 12.

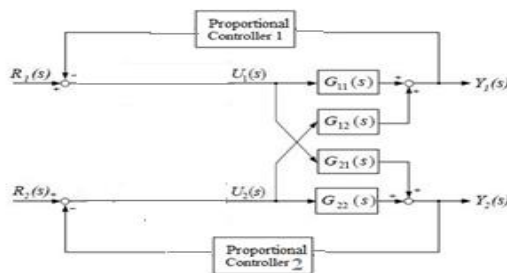


Fig 12. System with two first order delay free processes

The characteristic equation of the system without loop interactions is given by

For loop 1, $1 + K_{p1}G_{11} = 0$ (17)

For loop 2, $1 + K_{p2}G_{22} = 0$ (18)

Where, K_{p1} and K_{p2} are proportional control gains for respective loops. Suppose that two loops are interacting with interaction dynamics as G_{21} and G_{12} , have their characteristic equation as

$$(1 + K_{p1}G_{11})(1 + K_{p2}G_{22}) - K_{p1}G_{21}K_{p2}G_{12} = 0 \quad (19)$$

Based on the characteristic equation the interaction problem can be stated as equations (17) and (18) will be stable for a wider range of Proportional gains and equation (19) will not be stable for the same range due to loop interactions [4]. Interaction analysis reveals that proper choice of input output pairing can minimize interaction problems but for higher dimensioned systems this method seems to be tedious [4].

Our objective is to completely remove the effect of loop interactions. This can be achieved via compensation networks known as decouplers. Decouplers decompose a multi variable process into a series of independent single loop subsystems so that, complete or ideal decoupling will occur.

For example, consider a 2x2 system with decoupling network shown in Fig 13. Where, u_i is the input to the system after decoupling (which are the duty ratios), y_i = System output and G_{ij} = Transfer function of corresponding input output pair ($i=j=1,2$)

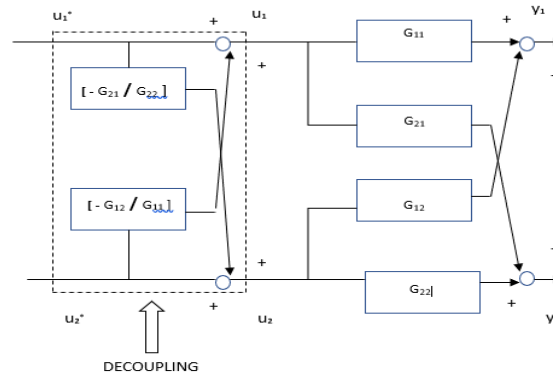


Fig 13 Decoupled network for a 2x2 system

From Fig 13,

$$u_1 = u_1^* + u_2^* [-G_{12} / G_{11}] \quad (20)$$

$$u_2 = u_2^* + u_1^* [-G_{21} / G_{22}] \quad (21)$$

Where u_i^* is the input to the decoupling network ($i=1,2$)

$$y_1 = u_1 G_{11} + u_2 G_{12} \quad (22)$$

Substituting (20) and (21) in (22) we get,

$$y_1 = u_1^* G_{11} - u_1^* [G_{21} / G_{22}] G_{12} \quad (23)$$

From (23) we understood that y_1 only depends on u_1^* and it is not affected when u_2^* changes.

Similarly, we get,

$$y_2 = u_2^* G_{22} - u_2^* [G_{12} / G_{11}] G_{21} \quad (24)$$

From (24) we can understand that y_2 only depends on u_2^* and it is not affected when u_1^* changes. That is the loop interactions are cancelled out through decoupling networks.

Applying this decoupling strategy to proposed three input converter decoupling transfer function for different modes are as follows,

$$G_{2 \times 2}^* = \begin{bmatrix} 1 & -g_{12} \\ -g_{21} & g_{11} \\ g_{22} & 1 \end{bmatrix} \text{ for mode 1}$$

$$G_{3 \times 3}^* = \begin{bmatrix} 1 & \frac{g_{13}g_{32} - g_{12}g_{33}}{g_{11}g_{33} - g_{13}g_{31}} & \frac{g_{12}g_{23} - g_{13}g_{22}}{g_{11}g_{22} - g_{12}g_{21}} \\ \frac{g_{23}g_{31} - g_{21}g_{33}}{g_{22}g_{33} - g_{23}g_{32}} & 1 & \frac{g_{13}g_{21} - g_{11}g_{23}}{g_{11}g_{22} - g_{12}g_{21}} \\ \frac{g_{21}g_{32} - g_{22}g_{31}}{g_{22}g_{33} - g_{23}g_{32}} & \frac{g_{12}g_{31} - g_{11}g_{32}}{g_{11}g_{33} - g_{13}g_{31}} & 1 \end{bmatrix}$$

for mode 2 and 3

This will result in an overall transfer function with respect to each control variable for different modes as

For mode 1,

$$\frac{y}{d_1} = g_{11} - g_{12} \frac{g_{21}}{g_{22}} \quad (25)$$

$$\frac{y}{d_2} = -g_{21} \frac{g_{12}}{g_{11}} + g_{22} \quad (26)$$



For mode 2,

$$\frac{y}{d_1} = g_{11} + g_{12} \frac{g_{13}g_{32} - g_{12}g_{33}}{g_{11}g_{33} - g_{13}g_{31}} + g_{13} \frac{g_{12}g_{23} - g_{13}g_{22}}{g_{11}g_{22} - g_{12}g_{21}} \quad (27)$$

$$\frac{y}{d_2} = g_{21} \frac{g_{23}g_{31} - g_{21}g_{33}}{g_{22}g_{33} - g_{23}g_{32}} + g_{22} + g_{23} \frac{g_{13}g_{21} - g_{11}g_{23}}{g_{11}g_{22} - g_{12}g_{21}} \quad (28)$$

$$\frac{y}{d_4} = g_{31} \frac{g_{21}g_{32} - g_{22}g_{31}}{g_{22}g_{33} - g_{23}g_{32}} + g_{32} \frac{g_{12}g_{31} - g_{11}g_{32}}{g_{11}g_{33} - g_{13}g_{31}} + g_{33} \quad (29)$$

For mode3,

$$\frac{y}{d_1} = g_{11} + g_{12} \frac{g_{13}g_{32} - g_{12}g_{33}}{g_{11}g_{33} - g_{13}g_{31}} + g_{13} \frac{g_{12}g_{23} - g_{13}g_{22}}{g_{11}g_{22} - g_{12}g_{21}} \quad (30)$$

$$\frac{y}{d_2} = g_{21} \frac{g_{23}g_{31} - g_{21}g_{33}}{g_{22}g_{33} - g_{23}g_{32}} + g_{22} + g_{23} \frac{g_{13}g_{21} - g_{11}g_{23}}{g_{11}g_{22} - g_{12}g_{21}} \quad (31)$$

$$\frac{y}{d_3} = g_{31} \frac{g_{21}g_{32} - g_{22}g_{31}}{g_{22}g_{33} - g_{23}g_{32}} + g_{32} \frac{g_{12}g_{31} - g_{11}g_{32}}{g_{11}g_{33} - g_{13}g_{31}} + g_{33} \quad (32)$$

Converter model together with derived decoupling network shown in different modes in Fig 14.

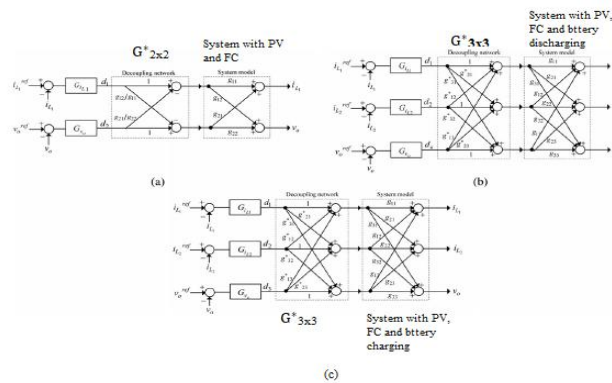


Fig 14. Converter model together with derived decoupling network for (a) Mode 1 (b) Mode 2 (c) Mode 3

From the transfer function equations (22) to (29) we can infer that coupling effects are not caused by nearby systems and hence the loop interactions in the system is getting cancelled out. Hence all the loops in the decoupled system can be considered as a single independent loop which allows implementation of independent controllers for each loop.

VI. SIMULATION OF PROPOSED SYSTEM

A three input DC-DC converter fed BLDC motor is simulated using MATLAB R2016a. PV, hydrogen FC and lead acid battery are supplying power to the load. For simulation equation modelled PV panel is used in order to create actual practical situations.

Simulation parameters of three input DC-DC converter are included in Table 1.

Table 1 Simulation parameters of three input DC-DC converter

Input voltage V_1	110V
Input voltage V_2	80V
Inductor $L_1 = L_2$	4mH
Capacitor C	220 μ F
Impedance Z	103 Ω
Switching frequency	20KHz
Irradiance of PV panel	1000W/m ²
Temperature of PV panel	25degree kelvin



Simulations are run with and without decoupling network for 1.5 sec. Closed loop simulation circuit diagram with decoupled network is shown in Fig 15 (a) and (b).

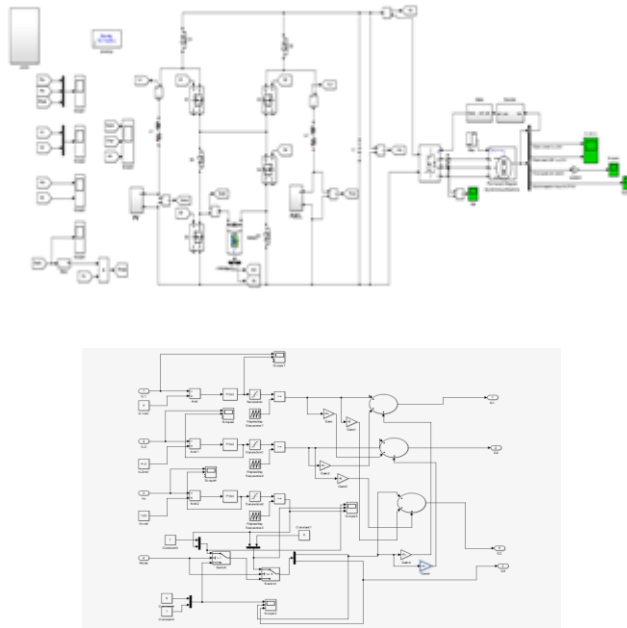
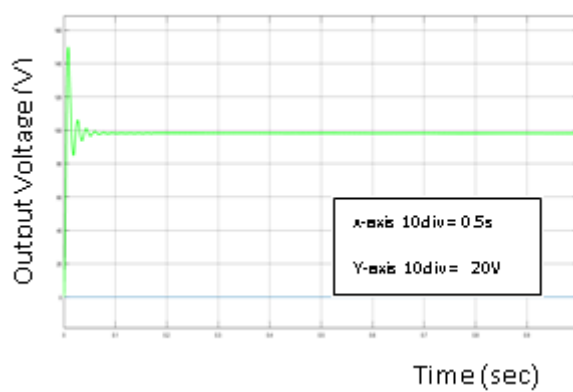


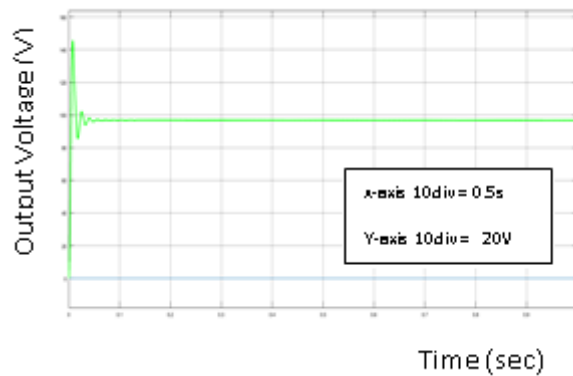
Fig 15(a) Simulation circuit diagram for three input DC-DC converter fed BLDC motor (b) Control circuit

Output Voltage of three input DC-DC converter during different modes of operations in open loop are shown in Fig 16 (a) (b) and (c).

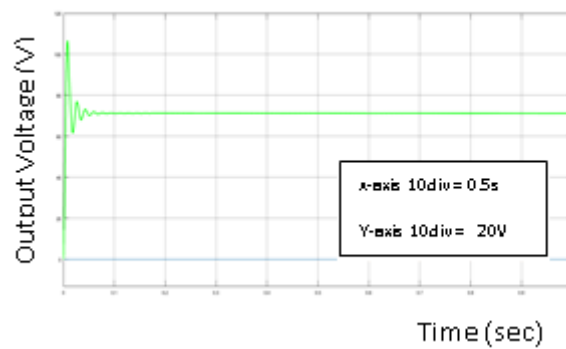
Mode 1:



(a)



(b)



(c)

Fig 16 (a) (b) (c) Output Voltage of three input DC-DC converter in open loop (a) Mode 1 (b) Mode 2 (c) Mode 3

It is inferred that without decoupling network the system with proposed DC-DC converter is not capable of providing desired response and transients are more. With decoupling network, the simulations are carried out with the same environment and the results obtained are provided in Fig 17.

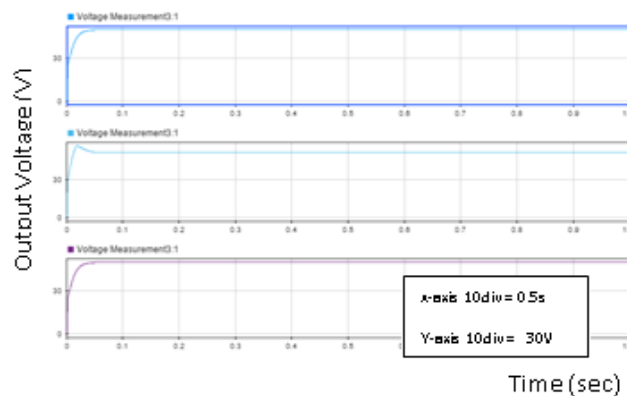


Fig 17. Output voltage in different modes of operations

It is observed that the output response obtained is very nearer to the expected values of 55V. As the proposed converter with decoupling converter has to supply the r BLDC motor of EV, the transient performance is to be studied. The transient parameters of the system with and without decoupling network listed in Table 2



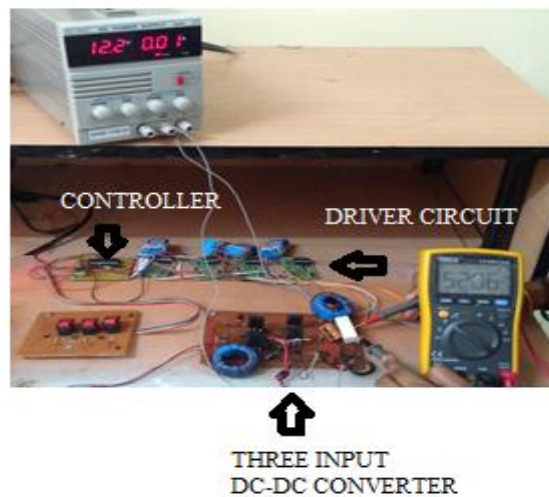
Table 2 Transient parameters of the system with and without decoupling network

Operations	Rise time(s)	Peak overshoot (%)	Settling time(s)
With Decoupling network	0.033	12.07	0.12
Without Decoupling network	0.04	52.74	0.28

On comparing the transient parameters of the proposed system with non-decoupled system, the rise time is 0.33s, peak overshoot is 12.07% and settling time is 0.12s, which is an improved value. Thus, MIC with decoupling network is preferred as it cancels the loop interactions making the system faster with better transient performance.

In order to validate this simulation results a hardware prototype is made results are produced. The results from hardware is comparable with the simulation which confirms the success of the new converter.

Hardware circuit:



Output Voltage obtained in 3 operating modes:



VII. CONCLUSION

Now a day's India government is proposing schemes to increase the production and use of EVs. Here a three input DC-DC converter with renewable input is proposed to make EVs more reliable. But with multiple inputs loop interactions will occur which will affect the overall performance of the vehicles. To reduce the effect, decoupling networks are



recommended. Simulation and hardware results reveals that decoupling networks cancels out the loop interactions and enhance the overall performance of the system.

REFERENCES

- [1] F. Nejabatkhah, S. Danyali, S. Hosseini, M. Sabahi and S. Niapour, “Modeling and Control of a New Three-Input DC–DC Boost Converter for Hybrid PV/FC/Battery Power System,” *IEEE Trans. Power Electron.*, vol. 27, no. 5, pp. 2309-2324, May. 2012
- [2] K Hirachi , M Yamanaka, T Takada, T Mii, M Nakaoka, “Feasible development of multi-functional bidirectional converter for solar photovoltaic generating system incorporating storage batteries” *IEEE Power electronic specialist conference*, 1995, vol.1, pp536-541
- [3] S Sopotpan, P Changmoang, P Panyakeow, “PV systems with/without grid backup for housing applications” *IEEE photovoltaic specialist conference sept 2000*
- [4] K.Warwick and D. Rees, *Industrial Digital Control Systems* (IEE Control Engineering Series 37). Stevenage, U.K: Peregrinus, 1988
- [5] B Ozpineci, LM Tolbert, D Zhong, “Multiple input converters for fuel cell” in proc. Industry application conference,2004.
- [6] RU Haque, MT Iqbal, JE Quaicoe, “Sizing , dynamic modelling and power electronics of a Hybrid energy system” , IEEE Canadian conference on electrical and computer engineering, Ottawa, May 2006.
- [7] AD Napoli, F Cresimbini , FG Capponi, L Solero, “Control strategy for multi-input DC-DC Power Converters for hybrid vehicle propulsion system,” IEEE Industrial electronics international symposium, vol3, May 2002.
- [8] L Solero, A Lidozzi, JA Pomilio, “ Design of multiple input power converter for hybrid vehicles”, IEEE Industrial electronics international symposium, vol3, May 2002.
- [9] L Solero, A Lidozzi, “Power balance control of multiple-input DC-DC power converter for hybrid vehicles”, IEEE Industrial electronics international symposium, vol3, May 2002.
- [10] B Ozpineci, LM Tolbert, D Zong, “Optimum fuel cell utilization with multi level inverters”, Power electronic specialist conference, vol6 2004
- [11] YM Chen, YC Liu, FY Wu, “Multi-input DC-DC converter based on multi winding transformer for renewable energy applications” IEEE Transaction on industrial applications vol 38.
- [12] YM Chen, YC Liu, FY Wu, TF Wu, “Multi-input DC-DC converter based on the flux additivity”, IEEE Proc. Industry applications conference vol 3 sept 2001.
- [13] Y Chen, Y Liu, ”Development of multi port converters for hybrid wind photovoltaic power system”, IEEE Electrical and electronic technology proceedings of international conference vol 2.
- [14] H Shiji, K Harada, Y Ishihara, T Todaka, G Alsamora, “ A zero-voltage- switching bidirectional converter for PV system”, IEEE telecommunication energy conference.
- [15] H Tao, A Kotsopoulos, JL Duarte, MAM Hendrix, “Multi-input bidirectional DC-DC Converter combining DC-link and magnetic coupling for fuel cell systems”, Industry appliction conference vol 3.
- [16] H Tao, A Kotsopoulos, JL Duarte, MAM Hendrix, “Family of multi port bidirectional DC-DC converter”, IEEE proc. Electric power applications vol 153.
- [17] Karteek Gummi, “ Derivation of new double input DC-DC converter using the building block methodology.
- [18] Y. Ch. Liu and Y.M. Chen, “A systematic approach to synthesizing multi-input DC–DC converters,” *IEEE Trans. Power Electron.*, vol. 24, no. 1,pp. 116–127, Jan. 2009.
- [19]MT Tham, “ Multi variablecontrol: An introduction to decoupling control”, An introduction to decoupling control/MTT/July 1999.
- [20]Fundamentals of Power Electronics, Robert W Ericson.
- [21] Zh. Qian, O. A. Rahman, H. A. Atrash, and I. Batarseh, “Modeling and control of three-port DC/DC converter interface for satellite applications,”*IEEE Trans. Power Electron.*, vol. 25, no. 3, pp. 637–649, Mar. 2010.